HAL
archives-ouvertes.fr

Elasticity of AlFeO(3) and FeAlO(3) perovskite and post-perovskite from first-principles calculations

Razvan Caracas

▶ To cite this version:

HAL Id: hal-00676913
https://hal.archives-ouvertes.fr/hal-00676913

Submitted on 6 Mar 2012

Elasticity of AlFeO₃ and FeAlO₃ perovskite and post-perovskite from first-principles calculations

R. Caracas[1]

[1]   We use state-of-the-art *ab initio* calculations based on the generalized gradient approximation of the density functional theory in the planar augmented wavefunction formalism to determine the elastic constants tensor of perovskite and post-perovskite with formulas AlFeO₃ and FeAlO₃ in which Fe or Al respectively occupy only octahedral sites, for the stable magnetic configurations. The phase transition between perovskite and post-perovskite is associated with a site exchange, during which Fe from the inter-octahedral site in perovskite moves into the octahedral site in post-perovskite. Following this transition path the elastic moduli show positive jumps, considerably larger than for MgSiO₃. The phase transition is marked by a positive jump of 0.04 km/s (0.33%) in the velocity of the compressional waves and by a negative jump of -0.15 km/s (-1.87%) in shear wave velocity. We find that the effects of the Mg + Si <=> Al + Fe substitution on the seismic properties of MgSiO₃ perovskite and post-perovskite depend on the crystallography of the substitution, namely the position the exchanged cations take in the structure. **Citation:** Caracas, R. (2010), Elasticity of AlFeO₃ and FeAlO₃ perovskite and post-perovskite from first-principles calculations, *Geophys. Res. Lett.*, *37*, L20306, doi:10.1029/2010GL044404.

1. Introduction

[2]   In the Earth's lower mantle, the most abundant silicate phase, both in perovskite (pv) and its high-pressure polymorph, post-perovskite (ppv) structures, is not pure MgSiO₃, but contains a certain amount of ferrous iron, ferric iron and aluminum as major substituents for Mg and Si. The exact proportion of each is still a matter of debate and obviously depends on a variety of factors, like local mantle conditions, temperature and pressure, mineralogical and petrological history, etc. An improved description should be obtained in a multidimensional system whose major components are MgSiO₃-FeSiO₃-FeAlO₃-AlFeO₃-Al₂O₃-Fe₂O₃. Realistic compositions would fall close to MgSiO₃ but will not be pure [*Anderson*, 1983].

[3]   Although pure AlFeO₃ composition is highly unlikely to exist, certain amounts of Al and Fe³⁺ are most certainly present in both pv and ppv in double substitution to Mg and Si. Consequently this substitution can change the thermodynamic conditions of the phase transition, modify the seismic properties, or affect the partitioning of elements or the spin state of iron.

[4]   In a previous computational study [*Caracas*, 2010] we analyzed the relative static stability of pv and ppv in this system. We treated only ordered stoichiometric structures and showed that the transition from pv to ppv involves an exchange of cation sites. We adopted a notation based on crystallochemistry: AlFeO₃ denotes the structure where Fe occupies the octahedral site and FeAlO₃ denotes the situation where Al occupies the octahedral space. At low pressure the stable phase is FeAlO₃ pv and above 90 GPa the stable phase is AlFeO₃ ppv, both in antiferromagnetic configuration. If the cation exchange fails to occur then the high-spin antiferromagnetic FeAlO₃ pv can metastably exist up to pressures beyond the Earth's mantle limit.

[5]   Most of the previous experimental studies on this system focused on the mechanism of incorporation of ferric iron in pv and on the possible role played by aluminum [e.g., *Andrault et al.*, 2001; *Daniel et al.*, 2004; *Nishio-Hamane et al.*, 2008]. They showed that there is a direct correlation between the amount of Al and Fe³⁺ that can be dissolved in MgSiO₃ pv, and that Al occupies preferentially the octahedral sites. More recent experiments addressing the transition from pv to ppv showed that the addition of Al and Fe³⁺ increases the transition pressure [*Andrault et al.*, 2008], in contradiction with the static theoretical findings for pure Al,Fe³⁺ oxide [*Caracas*, 2010]. The discrepancy between the theoretical and the experimental studies arises mainly from the sluggish perovskite - post-perovskite phase transition, which is associated with the Al and Fe³⁺ exchanging crystallographic sites. This involves breaking strong interatomic bonds that are hard to achieve, which in turn results in strong kinetic effects that delay the experimental transition pressure with respect to the theoretical one.

[6]   In this study we focus on the elastic and seismic properties. We determine the full elastic constants tensor and derive the corresponding bulk seismic properties for both crystallochemical cases for both structures. We consider only the stable magnetic configurations in each case: antiferromagnetic for FeAlO₃ pv and AlFeO₃ ppv and ferromagnetic for AlFeO₃ pv and FeAlO₃ ppv with net residual magnetic moments of respectively 4 and 8 magneton Bohrs per primitive unit cell.

2. Computational Details

[7]   We perform static (i.e., T = 0K) first-principles calculations based on the planar augmented wavefunctions (PAW) formalism [*Blochl*, 1994] within the generalized gradient approximation [*Perdew et al.*, 1996] of the density functional theory, as implemented in the ABINIT code [*Torrent et al.*, 2008; *Gonze et al.*, 2002]. We sample the electronic density in the reciprocal space (in the first Brillouin zone) using $6 \times 6 \times 6$ and $6 \times 6 \times 4$ grids of special high-

[1]Laboratoire de Sciences de la Terre, UMR 5570, Ecole Normale Supérieure de Lyon, CNRS, Lyon, France.

Table 1. Density in Grams per Cubic Centimeter at Several Pressures in the Two Crystallochemical Cases[a]

P	$FeAlO_3$ PV	$AlFeO_3$ PV	$FeAlO_3$ PPV	$AlFeO_3$ PPV
0	4.633	4.800		
30	5.158	5.406		
60	5.652	5.789	5.685	5.928
90	6.030	6.215	6.037	6.526
120	6.368	6.537	6.347	6.592
150	6.675	6.828	6.626	6.870

[a]Pressure values are in GPa. PV and PPV denote respectively the perovskite and post-perovskite structures. The jump at the phase transition pressure (90 GPa) between $FeAlO_3$ PV and $AlFeO_3$ PPV is almost 0.5 g/cm^3.

symmetry **k** points [*Monkhorst and Pack*, 1976] for the pv and ppv structures, respectively. We employ a 16 Ha (1 Ha = 27.2116 eV) kinetic energy cut-off for the wavefunctions on the coarse mesh and a 36 Ha cut-off for the wavefunctions on the finer grid inside the PAW spheres. This set of parameters ensures an accuracy of the calculation better than 1 GPa in pressure and 1 mHa/unit cell in energy.

[8] A drawback of our calculations might be their static character. But many of the physical properties of geophysical interest, like elasticity and compressibility, depend in a first approximation on the specific volume [*Wentzcovitch et al.*, 2004], which is shifted in static calculations by a few percent relative to the experimental values at higher temperature; but the shift arises in a consistent manner. This makes the static (0K) elastic data extremely useful. As GGA tends to overestimate the experimental ambient volume and LDA to underestimate it, results in GGA are comparable, though not similar, to thermal LDA [*Payne et al.*, 1992]. Moreover for this particular system the primary effect of temperature would be in affecting the Fe/Al site occupancy. A second limitation, the use of standard GGA rather than more sophisticated ways of treating strongly correlated electrons, like the GGA + U, is less important since the +U formalism is expected to have little effect on mechanical properties. This arises from the shift of the total energy in GGA + U relative to GGA, which is commensurable to the U parameter and weakly dependent on volume. Consequently derivatives of the GGA + U energy would not drastically differ from the derivatives of the GGA energy at a given density.

[9] First we fully relax the crystal structure in the desired magnetic configuration at a given target pressure, *i.e.* under respective symmetry constraints we allow the atoms to move to minimize the residual forces and the unit cell to distort to eliminate the non-hydrostatic stresses. Then we apply positive and negative strains of 1% and 2%. For each case we allow only the atoms to relax and we measure the residual stresses. Then we obtain the elastic constants tensor using the stress-strain relation in the linear limit.

[10] Both structures are orthorhombic and have nine independent, non-zero elastic constants, which in matrix (Voigt) notation are: C_{11}, C_{22}, C_{33}, C_{12}, C_{13}, C_{23}, C_{44}, C_{55}, C_{66}. The first three are pure-strain and the last three pure shear. We consider homogenous aggregates and use standard expressions for the bulk (K) and shear (G) elastic moduli, and for the compressional (Vp) and shear (Vs) seismic wave velocities.

3. Results and Discussion

[11] Table 1 summarizes the densities of the pv and ppv structures in the two crystallochemical cases. For both structures the arrangement with Fe occupying the octahedral site yields larger densities, partly because of the lower value of the magnetic spin. At the transition between the stable thermodynamical phases, $FeAlO_3$ pv and $AlFeO_3$ ppv the density difference is almost 0.5 g/cm^3, corresponding to 8.23% positive jump.

[12] The elastic constants of pv at several pressures are listed in Table 2. The compressibility of the two crystallochemical cases is different and in general the pressure enhances these differences. C_{12}, C_{13} and C_{23} and the pure strain elastic constants C_{11} and C_{22} are larger in $AlFeO_3$ than in $FeAlO_3$. C_{33} and all the three pure shear constants are larger in $FeAlO_3$. This results in opposite trends for the bulk and the shear elastic moduli (for homogeneous aggregates) with K smaller and G larger in $FeAlO_3$. pv in $AlFeO_3$ configuration shows a pronounced elastic softening at ambient pressure conditions with C_{66} only 3 GPa and C_{44} = 54 GPa. This yields a smaller than expected shear modulus. The poisson ratio also shows an anomaly with its largest value at

Table 2. Elastic Constants of Perovskite at Several Pressures in the Two Crystallochemical Cases[a]

	AlFeO₃						FeAlO₃					
P	0	30	60	90	120	150	0	30	60	90	120	150
C_{11}	397	532	647	753	895	983	421	513	609	698	820	883
C_{22}	478	650	814	939	1074	1176	477	625	749	893	1020	1116
C_{33}	256	437	586	712	825	922	314	446	590	728	871	953
C_{12}	159	288	404	529	638	713	205	239	333	410	497	575
C_{13}	136	239	319	407	497	577	159	227	290	347	428	490
C_{23}	150	245	342	438	537	624	184	249	319	393	465	528
C_{44}	54	127	171	218	255	278	126	170	204	247	284	307
C_{55}	103	118	119	132	147	155	101	114	136	153	171	168
C_{66}	3	39	78	95	126	142	97	142	173	201	225	236
K	216	345	456	563	672	757	250	331	422	508	606	676
G	89	202	265	302	349	374	216	282	336	390	442	455
Y	236	506	666	768	893	963	503	659	796	932	1066	1116
η	0.32	0.26	0.26	0.27	0.28	0.29	0.17	0.17	0.19	0.19	0.21	0.23

[a]All values are in GPa, except for ν, which is adimensional.

Table 3. Elastic Constants of Post-Perovskite at Several Pressures in the Two Crystallochemical Cases[a]

	AlFeO$_3$			FeAlO$_3$		
P	90	120	150	90	120	150
C$_{11}$	865	955	1091	860	1010	1132
C$_{22}$	865	993	1125	767	862	962
C$_{33}$	891	1028	1165	868	1015	1164
C$_{12}$	456	549	647	412	511	602
C$_{13}$	367	439	518	375	450	534
C$_{23}$	472	569	672	450	543	641
C$_{44}$	209	223	245	144	170	207
C$_{55}$	103	128	171	91	114	149
C$_{66}$	342	387	444	291	335	370
K	578	675	782	552	654	756
G	407	454	522	349	403	463
Y	988	1113	1280	865	1003	1153
η	0.22	0.23	0.23	0.24	0.24	0.25

[a]All values are in GPa, except for ν, which is adimensional.

0 GPa. However at ambient conditions pv is not thermodynamically stable.

[13] The pressure variation of the elastic constants of ppv is listed in Table 3. The elastic properties of the two crystallochemical cases are similar. The major differences are in the C$_{11}$ and C$_{22}$ constants: the first one is larger in FeAlO$_3$ and the second one in AlFeO$_3$. The differences are accentuated by pressure. The behavior of the pure shear constants is different: C$_{44}$ is larger in AlFeO$_3$, C$_{66}$ is larger in FeAlO$_3$ and C$_{55}$ is roughly the same in the two cases. The bulk moduli differ by about 20 GPa and the shear moduli by about 50 GPa both larger for AlFeO$_3$. Both the Young modulus and the Poisson ratio are smaller than most of other perovskites [*Caracas and Cohen*, 2007; *Caracas et al.*, 2010].

[14] At the thermodynamic transition accompanied by the cationic site exchange at 90 GPa [*Caracas*, 2010] the bulk modulus has a positive jump of 70 GPa (13.8%) and the shear modulus a positive jump of 16 GPa (4.2%) as shown in Figure 1. These values are larger than at the same transition in pure MgSiO$_3$ [*Caracas and Cohen*, 2005].

[15] Figure 2 shows the variation of the seismic wave velocities with respect to pressure for all the cases consid-

ered here. In pv the velocities of the FeAlO$_3$ crystallochemical arrangement are larger than those of the AlFeO$_3$ one by almost 0.6 km/s for Vp and about 1 km/s for Vs in the 60–120 GPa pressure range. In ppv the trend is reversed with Vp larger in AlFeO$_3$ by 0.12–0.27 km/s and Vs larger in AlFeO$_3$ by 0.29–0.36 km/s in the 60–150 GPa pressure range. The velocities of the pv and ppv structures have different slopes under pressure, regardless of the crystallochemistry. The slope of Vp changes from 0.022 km/s/GPa for pv to 0.027 km/s/GPa in ppv and the slope of Vs changes from 0.010 km/s/GPa for pv to 0.016 km/s/GPa in ppv (For Vp of AlFeO$_3$ we used for the fit only the 60–120 GPa pressure range because of the low-pressure softening). This behavior stems from different equations of state, with larger compressibility and larger density for the ppv.

[16] In Figures 1 and 2 we outline with arrows the path followed by the system at thermodynamic equilibrium, namely during a phase transition at 90 GPa from the FeAlO$_3$ pv to AlFeO$_3$ ppv. The change in Vp is small: a positive jump of 0.043 km/s corresponding to 0.33% of the velocity in pv at the transition pressure. The change in Vs is larger and of opposite sign: a negative jump of −0.15 km/s corresponding to −1.87% of the shear velocity in pv. At larger pressure, namely at 120 GPa, the difference in Vp between the two structures and crystallochemical cases increases to 0.24 km/s, corresponding to 1.75% relative difference, while the difference in Vs vanishes.

[17] Of course these values are not meaningful by themselves for the lower mantle, but they should be used to apply corrections to MgSiO$_3$ case, alongside FeSiO$_3$ or Al$_2$O$_3$.

[18] Static calculations for the pure MgSiO$_3$, FeSiO$_3$ and Al$_2$O$_3$ compositions [e.g., *Oganov and Ono*, 2004; *Caracas and Cohen*, 2005; *Tsuchiya and Tsuchiya*, 2006; *Stackhouse et al.*, 2005, 2006] and summarized by *Caracas and Cohen* [2007] show that MgSiO$_3$ has the largest seismic wave velocities, both for compressional waves and for shear waves. Any addition of ferrous iron or aluminum or a combination thereof decrease both Vp and Vs for both pv and ppv. Seismic anisotropy instead does not present clear trends and adding Fe^{2+} or Al [*Caracas and Cohen*, 2007] or allowing for the iron spin to change [*Caracas et al.*, 2010] can yield
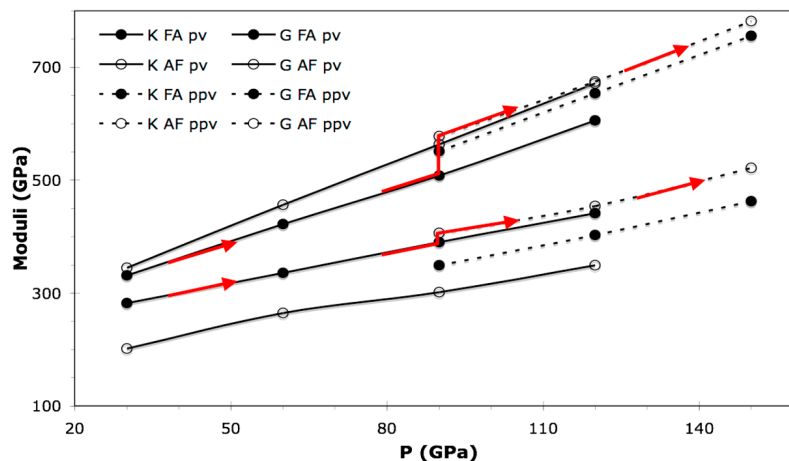

Figure 1. Pressure variation of the elastic moduli of perovskite and ppv in the two crystallochemical cases. The notations are as follows: AF = AlFeO$_3$, FA = FeAlO$_3$, pv = perovskite, ppv = post-perovskite.
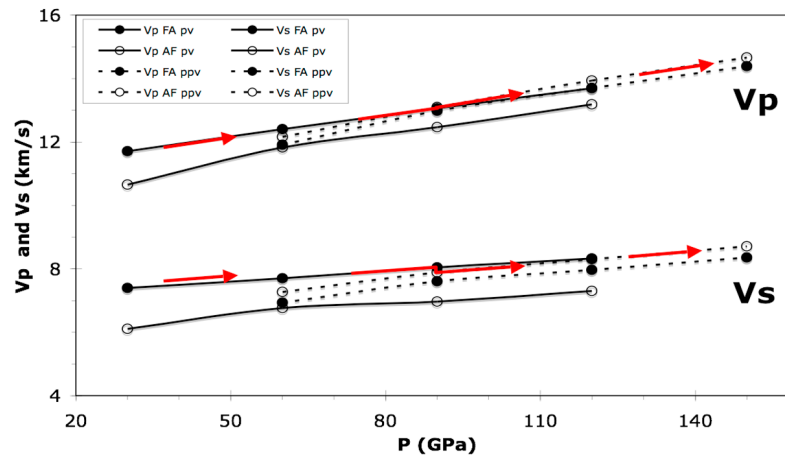
Figure 2. Pressure variation of the seismic wave velocities of perovskite and post-perovskite in the two crystallochemical cases. The notations are as follows: AF = AlFeO$_3$, FA = FeAlO$_3$, pv = perovskite, ppv = post-perovskite.

different anisotropy patterns. For a Mg-rich silicate composition [*Caracas and Cohen*, 2007] compatible with an average pyrolitic mantle composition [*Kesson et al.*, 1998; *Murakami et al.*, 2005] and assuming that all Fe in the silicate is ferrous, the differences between seismic velocities of postperovskite and perovskite structures are positive for Vp at pressures above 112 GPa and for Vs at pressures above 86 GPa: at 100 GPa the differences are −0.2% in Vp and +0.7% in Vs; at 130 GPa the differences are +0.5% in Vp and +2% in Vs. The only static elastic calculations so far on perovskite (Mg$_{0.9375}$Fe$_{0.0625}$) (Si$_{0.9375}$Al$_{0.0625}$)O$_3$ compositions with ferric iron on the Mg site and aluminum on the Si site, in several substitutional patterns *Li et al.* [2005] showed a decrease of the velocities. Moreover the velocities varied within narrow ranges for both Vp, 14.06–14.09 km/s, and Vs, 7.53–7.55 km/s, regardless of the geometric arrangement of the substitution.

[19] In case of mixed addition of both Al and ferric Fe, our results summarized in Figure 2 and Table 4 shows that the trends are different than in the case of the substitutions with Al-only and/or Fe^{2+}. If we refer in particular to the values at 120 GPa (summarized by *Caracas and Cohen* [2007, Table 2]) the Mg + Si < = > Al + Al substitution decreases Vp of pure MgSiO$_3$ in both crystallochemical cases and for both pv and ppv. Moreover it is interesting to note that the quantitative behavior of FeAlO$_3$ is similar to the one of Al$_2$O$_3$. One could cautiously speculate that the presence of Al in the octahedral framework is determinant to the compressibility pattern and that the cations on the interoctahedral site play a minor role. At 120 GPa, for Vs the Al-Fe substitution in pv (Fe on octahedral site; Vs = 7.31 km/s) and the Al-Fe substitution in ppv (Fe on octahedral site; Vs = 7.97 km/s) tend to lower or at least keep constant the Vs of MgSiO$_3$ (Vs = 7.7 km/s for pv and Vs = 7.8–8.3 km/s for ppv). But the Fe-Al substitution (Al on octahedral site) in pv tends to increase the shear velocity, with Vs for pure FeAlO$_3$ of 8.33 km/s at 120 GPa. The Al-Fe substitution in ppv (Al on octahedral site) also tends to increase Vs of MgSiO$_3$, with Vs for pure AlFeO$_3$ ppv of 8.30 km/s at 120 GPa.

[20] Experimental Brillouin measurements on pure MgSiO$_3$ perovskite and post-perovskite [*Murakami et al.*, 2007]

show similar velocity jumps at the transition between the two structures and similar pressure dependencies. But pure Mg-composition are not enough to explain the seismic discontinuity at the top of the D″ layer (at 120–130 GPa). The velocity jumps for homogeneous MgSiO$_3$ aggregates are too small and various mechanisms [*Wookey et al.*, 2005], including lattice-preferred orientation (LPO) [*Merkel et al.*, 2006] have been proposed to match mineral physics with seismology. However a viable alternative to LPO or at least a partial alternative that would reduce the constraints on LPO would be the change in chemistry, namely the presence of either ferrous [*Caracas and Cohen*, 2007] or ferric (this study) iron.

[21] Consequently, the theoretical values of this study are important as they show that (i) the thermodynamically-favorable substitution tends to decrease Vp and increase Vs and (ii) the influence of the Mg + Si < = > Al + Fe substitution on the seismic properties of both pv and ppv is strongly dependent on the substitution mechanism and the ordering of the cations on the crystallographic sites. Thus these results are part of the greater puzzle represented by the pv - ppv transition and represent critical information necessary to model the lowermost part of the Earth's mantle at realistic chemical compositions. A full integration of all the chemical information into a general seismic model of pv and ppv will be the subject of a future study.

Table 4. Seismic Wave Velocities of Perovskite and Post-Perovskite at Several Pressures in the Two Crystallochemical Cases[a]

P	30	60	90	120	150
Vp FeAlO$_3$ pv	11.71	12.41	13.06	13.70	
Vs FeAlO$_3$ pv	7.40	7.71	8.04	8.33	
Vp AlFeO$_3$ pv	10.66	11.82	12.47	13.19	
Vs AlFeO$_3$ pv	6.11	6.76	6.97	7.31	
Vp FeAlO$_3$ ppv		11.92	12.98	13.70	14.39
Vs FeAlO$_3$ ppv		6.94	7.61	7.97	8.36
Vp AlFeO$_3$ ppv		12.16	13.10	13.94	14.66
Vs AlFeO$_3$ ppv		7.27	7.89	8.30	8.71

[a]Pressure (P) is in GPa and velocities in km/s; pv, perovskite; ppv, post-perovskite.

References

Anderson, D. (1983), Chemical composition of the mantle, *J. Geophys. Res.*, *88*, B41–B52.

Andrault, D., N. Bolfan-Casanova, and N. Guignot (2001), Equation of state of lower mantle (Al,Fe)-MgSiO$_3$ perovskite, *Earth Planet. Sci. Lett.*, *193*, 501–508.

Andrault, D., M. Munoz, N. Bolfan-Casanova, N. Guignot, J. Perrilat, G. Aquilanti, and S. Pascarelli (2008), The perovskite to post-perovskite phase transition in Al-bearing (Mg,Fe)SiO$_3$: A XANES in-situ analysis at the Fe K-edge, *Eos Trans. AGU*, *89*, Fall Meet. Suppl., Abstract MR42A-02.

Blochl, P. E. (1994), Projector augmented-wave method, *Phys. Rev. B*, *50*, 17,953–17,979.

Caracas, R. (2010), Spin and structural transitions in AlFeO$_3$ and FeAlO$_3$ perovskite and post-perovskite, *Phys. Earth Planet. Inter.*, doi:10.1016/j.pepi.2010.06.001, in press.

Caracas, R., and R. E. Cohen (2005), Effect of chemistry on the stability and elasticity of the perovskite and post-perovskite phases in the MgSiO$_3$-FeSiO$_3$-Al2O$_3$ system and implications for the lowermost mantle, *Geophys. Res. Lett.*, *32*, L16310, doi:10.1029/2005GL023164.

Caracas, R., and R. E. Cohen (2007), Effect of chemistry on the physical properties of perovskite and post-perovskite, in *Post-Perovskite: The Last Mantle Phase Transition*, Geophys. Monogr. Ser., vol. 174, edited by K. Hirose et al., pp. 115–128, AGU, Washington, D. C.

Caracas, R., and R. E. Cohen (2008), Ferrous iron in post-perovskite from first-principles calculations, *Phys. Earth Planet. Inter.*, *168*, 147–152.

Caracas, R., D. Mainprice, and C. Thomas (2010), Is the spin transition in Fe^{2+}-bearing perovskite visible in seismology?, *Geophys. Res. Lett.*, *37*, L13309, doi:10.1029/2010GL043320.

Daniel, I., J. D. Bass, G. Fiquet, H. Cardon, J. Zhang, and M. Hanfland (2004), Effect of aluminium on the compressibility of silicate perovskite, *Geophys. Res. Lett.*, *31*, L15608, doi:10.1029/2004GL020213.

Gonze, X., et al. (2002), First-principles computation of material properties: The ABINIT software project, *Comput. Mater. Sci.*, *25*, 478–492.

Gonze, X., et al. (2005), A brief introduction to the ABINIT software package, *Z. Kristallogr.*, *220*, 558.

Hohenberg, P., and W. Kohn (1964), Inhomogenous electron gas, *Phys. Rev.*, *136*, 864B–871B.

Kesson, S. E., J. D. Fitz Gerald, and J. M. Shelley (1998), Mineralogy and dynamics of a pyrolite mantle, *Nature*, *393*, 252–255.

Li, L., J. P. Brodholt, S. Stackhouse, D. J. Weidner, M. Alfredsson, and G. D. Price (2005), Elasticity of (Mg, Fe)(Si, Al)O$_3$ perovskite at high pressure, *Earth Planet. Sci. Lett.*, *240*, 529–536.

Merkel, S., A. Kubo, L. Miyagi, S. Speziale, T. S. Duffy, H. Mao, and H.-R. Wenk (2006), Plastic deformation of MgGeO$_3$ post-perovskite at lower mantle pressures, *Science*, *311*, 644–646.

Monkhorst, H. J., and J. D. Pack (1976), Special points for Brillouin-zone integrations, *Phys. Rev. B*, *13*, 5188–5192.

Murakami, M., K. Hirose, N. Sata, and Y. Ohishi (2005), Post-perovskite phase transition and mineral chemistry in the pyrolitic lowermost mantle, *Geophys. Res. Lett.*, *32*, L03304, doi:10.1029/2004GL021956.

Murakami, M., S. V. Sinogeikin, J. D. Bass, N. Sata, Y. Ohishi, and K. Hirose (2007), Sound velocity of MgSiO$_3$ post-perovskite phase: A constraint on the D″ discontinuity, *Earth Planet. Sci. Lett.*, *259*, 18–23.

Nishio-Hamane, D., T. Nagai, K. Fujino, Y. Seto, and N. Takafuji (2005), Fe^{3+} and Al solubilities in MgSiO$_3$ perovskite: Implication of the Fe^{3+}AlO$_3$ substitution in MgSiO$_3$ perovskite at the lower mantle condition, *Geophys. Res. Lett.*, *32*, L16306, doi:10.1029/2005GL023529.

Oganov, A., and S. Ono (2004), Theoretical and experimental evidence for a post-perovskite phase in MgSiO$_3$ in the Earth's D″ layer, *Nature*, *430*, 445–448.

Payne, M. C., M. P. Teter, D. C. Allan, T. A. Arias, and J. D. Joannopoulos (1992), Iterative minimization techniques for ab initio total-energy calculations: Molecular dynamics and conjugate gradients, *Rev. Mod. Phys.*, *64*, 1045–1097.

Perdew, J. P., K. Burke, and M. Ernzerhof (1996), Generalized gradient approximation made simple, *Phys. Rev. Lett.*, *77*, 3865–3868.

Stackhouse, S., J. P. Brodholt, and G. D. Price (2005), High temperature elastic anisotropy of the perovskite and post-perovskite polymorphs of Al$_2$O$_3$, *Geophys. Res. Lett.*, *32*, L13305, doi:10.1029/2005GL023163.

Stackhouse, S., J. P. Brodholt, and G. D. Price (2006), Elastic anisotropy of FeSiO$_3$ end-members of the perovskite and post-perovskite phases, *Geophys. Res. Lett.*, *33*, L01304, doi:10.1029/2005GL023887.

Torrent, M., F. Jollet, F. Bottin, G. Zerah, and X. Gonze (2008), Implementation of the projector augmented-wave method in the ABINIT code: Application to the study of iron under pressure, *Comput. Mater. Sci.*, *42*, 337–351.

Tsuchiya, T., and J. Tsuchiya (2006), Effect of impurity on the elasticity of perovskite and postperovskite: Velocity contrast across the postperovskite transition in (Mg,Fe,Al)(Si,Al)O$_3$, *Geophys. Res. Lett.*, *33*, L12S04, doi:10.1029/2006GL025706.

Tsuchiya, T., J. Tsuchiya, K. Umemoto, and R. M. Wentzcovitch (2004), Phase transition in MgSiO$_3$ perovskite in the Earth's lower mantle, *Earth Planet. Sci. Lett.*, *224*, 241–248.

Wentzcovitch, R. M., B. B. Karki, M. Cococcioni, and S. de Gironcoli (2004), Thermoelastic properties of MgSiO$_3$-perovskite: Insights on the nature of the Earth's lower mantle, *Phys. Rev. Lett.*, *92*, 018501, doi:10.1103/PhysRevLett.92.018501.

Wookey, J., S. Stackhouse, J. M. Kendall, J. P. Brodholt, and G. D. Price (2005), Efficacy of the post-perovskite phase as an explanation for lowermost-mantle seismic properties, *Nature*, *438*, 1004–1007.

R. Caracas, Laboratoire de Sciences de la Terre, UMR 5570, Ecole Normale Supérieure de Lyon, CNRS, 46, allée d'Italie, F-69364 Lyon CEDEX 07, France. (razvan.caracas@ens-lyon.fr)